Hindawi Publishing Corporation
International Journal of Photoenergy
Volume 2013, Article ID 350698, 7 pages
http://dx.doi.org/10.1155/2013/350698

Research Article

Dyes Degradation with Fe-Doped Titanium Nanotube Photocatalysts Prepared from Spend Steel Slag

Chih Ming Ma,[1] Yu Jung Lin,[2] Ren Wei Shiue,[2] and Chang Tang Chang[2]

[1] *Department of Cosmetic Application and Management, St. Mary's Medicine Nursing and Management College, Number 100, Lane 265, Section 2, Sansing Road. Sansing Township, Yilan County 266, Taiwan*
[2] *Department of Environmental Engineering, National I-Lan University, Number 1, Section 1, Shen-Lung Road, Ilan 260, Taiwan*

Correspondence should be addressed to Chang Tang Chang; ctchang@niu.edu.tw

Received 22 January 2013; Revised 20 April 2013; Accepted 23 April 2013

Academic Editor: Jiaguo Yu

TiO_2 has been studied most commonly because it has high stability, nontoxicity, high catalytic activity, and high conductivity. Many studies have shown that TiO_2 would generate electron-hole pairs illuminated with UV and surround more energy than that before being illuminated. In this study, the titanium nanotube (TNT) photocatalysts were prepared to increase the surface area and adsorption capacity. The Fe TNT was also prepared from a slag iron since many slag irons cause waste treatment problems. In this study, a different Fe loading was also assessed since TNT doped with metals can be used to improve the degradation efficiency. Furthermore, five kinds of dye concentration, including 10, 20, 100, 200, and 400 ppm, and five kinds of Fe-doped content, including 0, 0.77, 1.13, 2.24, and 4.50%, were tested. Different kinds of reaction time and dye species were also assessed. In this result, Direct Black 22 was the most difficult to be degraded, although the concentration was decreased or the dose amount was increased. The degradation efficiency of 10 ppm Direct Black 22 was below 40% with 0.04 gL^{-1} TNT under 365 nm UV irradiation.

1. Introduction

About 15% of the total world production of dyes is lost during textile dyeing when dyes are released as textile effluents [1]. Dyes are widely used in the textile industry and cause polluted water. The disposal of this colored wastewater into the environment leads to many ecological problems as well as diminished natural aesthetics [2]. How to efficiently solve this urgent environmental issue has become a challenging and indispensable topic of modern research.

The traditional methods for treating dye wastewater include adsorption, coagulation, and biological treatment, but they do not have good performance [3]. In contrast, photocatalytic degradation is considered to be an efficient and economical alternative for controlling dye wastewater. Currently, several new photocatalysts, most impregnated with metal oxide and composite metal oxide semiconductors have been used to overcome the drawbacks of TiO_2, which has low surface area and adsorption capacity [4]. The photocatalysts commonly used are TiO_2, ZnO, WO_3, CdS, ZnS, $SrTiO_3$, and Fe_2O_3, with TiO_2 being frequently reported as the most active in organic degradation experiments [5]. For example, in suitable irradiation sunlight, using titanium dioxide can decrease costs significantly [6]. Photocatalysts have several obvious advantages in technique, including cleaner air, an extraction stream, and carbon adsorption. In these processes, oxygens occur $OH^{\bullet}$ hit, and a rate constant is higher than the oxidation of a normal state ten billion times. Ultraviolet irradiation can be obtained from sunlight or a simulated light source.

The photocatalytical activity of the S-TiO_2 photocatalyst at 400°C for the photodegradation of L-acid is better than that of pure TiO_2 [7]. A novel In^{3+}-doped TiO_2 and TiO_2/In_2S_3 nanocomposites for photocatalytic degradation of environmental pollutants and stoichiometric degradation of warfare agents is prepared using homogeneous hydrolysis with urea and thioacetamide [8]. Through high-energy ball-milling technique, the nanostructured (20 nm) TiO_2 photocatalysts with different quantities of Cr doping were synthesized for 3 hours [9]. Early studies primarily focused on TiO_2-based photocatalysts, though TiO_2 only responds

to ultravisible (UV) irradiation, which accounts for only about 4% of all solar energies which greatly hinders wider application [10].

In our experiment, TiO_2 was chosen for modification into TNT (titanium nanotube) because it shows relatively high chemical stability, exhibits high activity for photocatalysis, and is relatively inexpensive [11]. This study used hydrothermal methods to modify the titanium dioxide into TNT. The largest difference is in the structure and surface area. The former is a spherical particle with a surface area of 50 $m^2\,g^{-1}$. The latter is a mesoporous tube shape with a surface area of roughly 400 $m^2\,g^{-1}$. The surface area, closely related to adsorption efficiency, is about eight times that of TiO_2 manufactured using the hydrothermal method [12]. Further, TNT can simultaneously generate photodegradation and adsorption in wastewater. TNT has vast pore structures and large surface areas owing to its unique tubular nanostructure [13]. This mesoporous catalyst is suitable for treating high dye concentrations in wastewater.

In this study, TNT was doped with different Fe contents to increase its absorption visible light. The Fe was extracted from slag iron in steel plant to reuse the iron. The aim of this study was to investigate the performance of TNT and Fe TNT for methyl blue (MB), Direct Blue (DB22), and Reactive Black (RBK5) removal using a photocatalytic reaction. In particular, factors such as doped Fe content, light source, initial dye concentrations, and dye species were assessed to establish the optimum operating conditions. Furthermore, the reaction kinetics analysis was also investigated in this study.

2. Materials and Methods

2.1. Preparation of TNT. Commercial TiO_2 (P25) nanoparticles (5 g) were mixed in an aqueous 10 M NaOH solution and charged into a Teflon-lined autoclave. The autoclave was then oven-heated at 135°C for 3 days. The precipitate was filtered, and the pH value of the slurry was adjusted with a diluted 0.1 M HNO_3 by washing. The final products were obtained by filtration with subsequent drying at 100°C overnight. Finally, the TNT samples were obtained through calcination at the temperatures of 400°C.

2.2. Preparation of Fe TNT by Photodeposition. An appropriate amount of TNT suspension solution was weighed in a Pyrex glass container and then purged with nitrogen for 2 h to remove any dissolved oxygen (DO) from the solution. Then an appropriate amount of Fe solution was weighed and mixed with 10 mL methanol and dissolved in TNT solution. Photodeposition was performed for 12 h under a continuous nitrogen purge using a 254-nm ultraviolet light. Once the Fe-TNT suspension solution was formed, the subsequent clearing was applied using methods similar to those used with the TNT photocatalyst.

2.3. Characterization of TNT and Fe TNT. A UV spectrometer (Hitachi, U-3900) was applied to analyze the reflectance spectra of TNT samples, ranging from 200 nm to 800 nm in wavelength. High-resolution transmission electron microscopy (HR-TEM, JEOL, EM2100 High Resolution TEM) was used for morphological observations of the TNT. Specifically, surface areas and pore volumes of the derived nanotubes were determined by N_2 adsorption/desorption isotherm (Micromeritics, BET ASAP 2020N).

2.4. The Performance Assessment of TNT and Fe TNT. The photocatalytic degradation of MB, DB22, and RBK5 for initial concentrations (10, 20, 100, 200, and 400 ppm), Fe-doped content (0, 0.77, 1.13, 2.24, and 4.50%) and light source (254 nm UV, 365 nm UV, 380 nm, and 490 nm) was determined by means of UV-Vis spectrophotometer analysis through indication of color disappearance. A calibration curve of methyl blue solution was obtained at 600 nm wavelength in order to correlate the concentration of MB at different reaction times by converting the absorbance of the sample to MB concentration. During the reaction time the solutions were centrifuged at 300 rpm to mix the dye well.

2.5. Kinetics Analysis. Pseudo-first-order reaction kinetics is the most commonly used kinetic expression to explain the kinetics of the heterogeneous catalytic processes. The Pseudo-first-order expression that explains the kinetics of heterogeneous catalytic systems is given by (1) [14]

$$r = -\frac{dC}{dt} = \frac{K_r KC}{1 + KC}, \tag{1}$$

where K_r is the reaction rate constant ($\text{mol dm}^{-1}\,\text{min}^{-1}$), K is the adsorption coefficient of the reactant on catalyst $(\text{mol dm}^{-3})^{-1}$, and C is the concentration of the solute (ppm or mg L^{-1}).

Pseudo-first-order expression reduces to first-order equation when C is small:

$$-\ln\left(\frac{C}{Co}\right) = k_1 t, \tag{2}$$

where $k_1 = K_r K$.

Yielding half-life, $t_{1/2}$(min) can be calculated as below (Habibi et al., 2005) [15]:

$$t_{1/2} = \frac{0.693}{k_1}. \tag{3}$$

3. Results and Discussion

3.1. UV-Visible Spectrum. In order to determine the photo absorbance properties, the commercial Fe TNT and TNT were analyzed by UV-Vis for wavelengths of 200–800 nm. The band gap (E, eV) of the six samples was calculated by (4) [16] as follows:

$$E = \frac{1240}{\lambda}, \tag{4}$$

where λ is the wavelength of UV absorption thresholds.

After calculation, P25, TNT (0% Fe TNT), and 1.13% Fe TNT had band gaps of 3.20, 3.10, and 2.7 eV, respectively,

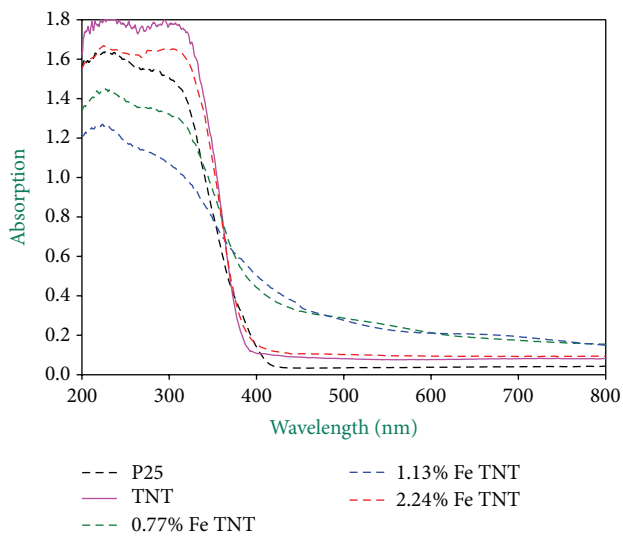

Figure 1: The UV absorption of P25 and Fe-doped TNT.

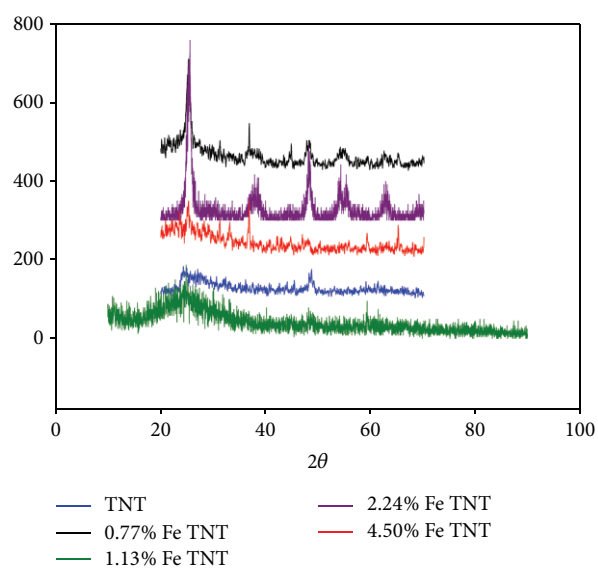

Figure 2: XRD spectra of the different Fe-doping catalyst.

as shown in Figure 1. The results showed that less energy was needed for reacting with pollutants with the 1.13% Fe TNT. It was found that the Fe-doped TiO_2 can get higher photocatalytic activity with visible light than that of P25. The differences between photocatalytic activity of different Fe-doped TiO_2 and pure TiO_2 were illustrated in Figure 7 and described later.

The TNT surface can be blocked with increasing the Fe content. It causes the surface of Fe TNT and band gap to decrease because the amount of Fe increases with increasing red shift.

X-ray diffraction was used to identify the Fe-TNT structures and compositions, as shown in Figure 2. From JCPDS-ICDD database, Fe particle was indentified with five root

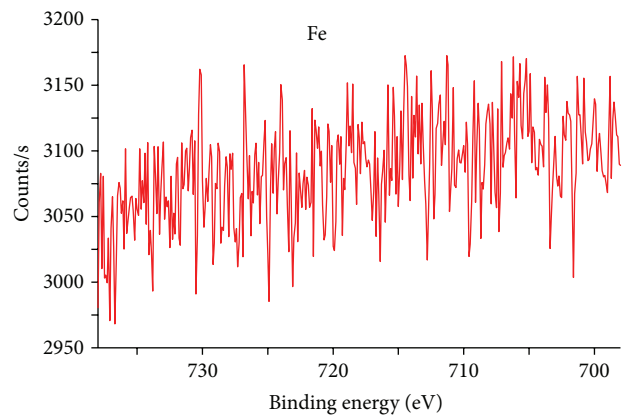

Figure 3: XPS spectra of the 4.50% Fe-TNT catalyst.

significantly diffraction peaks at (104), (110), (024), (116), and (214) crystal surface.

The peaks of Fe $2p^{3/2}$ can be decomposed into two contributions corresponding to the different oxidation of iron, respectively. The main contribution is attributed to Fe^{3+} ions (binding energy at 709.1 eV), and the other is to Fe^{2+} ion (binding energy at 710.9 eV) [17]. However, the Fe cannot be detected with no element diffraction peak since the Fe content is too small as shown in Figure 3.

The typical tube structure of the TNT was shown in the TEM image. The tube size, judged from the TEM image, ranged from 5–10 nm and was smaller than the results of Park et al. [18], but similar to the results of Song et al. [19]. The end of the tube was open, which is extremely critical for TNT absorption and photocatalysis ability [20]. This shows that the hydrothermal method successfully changed the p25 nanopowder into nanotubes. As observed in Figure 4, the nanotubes were scrolls which can be explained by the hydrothermal mechanism.

3.2. N_2 Adsorption and Desorption Analyzer. The catalyst surface area was determined by an accelerated surface area and porosimetry analyzer (ASAP 2000) from Micromeritics company using nitrogen at a constant temperature (−196°C). The data obtained from the N_2 adsorption and desorption analyzer showed that the surface area of the TNT was 331 $m^2\,g^{-1}$, which was larger than that of 4.50% Fe TNT.

3.3. Degradation of MB

3.3.1. The Effect of Initial Concentration. The temperature and catalysis loading were controlled at 25°C and 0.04 gL^{-1}, respectively, to test the effect of initial concentration. Five kinds of concentrations, including 10, 20, 100, 200, and 400 ppm (mg L^{-1}), were assessed to understand the effects of initial concentrations on the degradation of MB. The effect of initial concentration on degradation efficiency is shown in Figure 6.

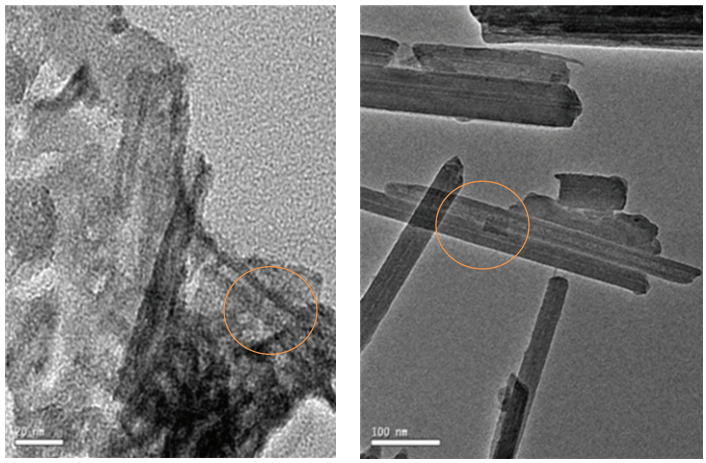

(a) (b)

Figure 4: TEM images of (a) TNT and (b) 2.24% Fe TNT.

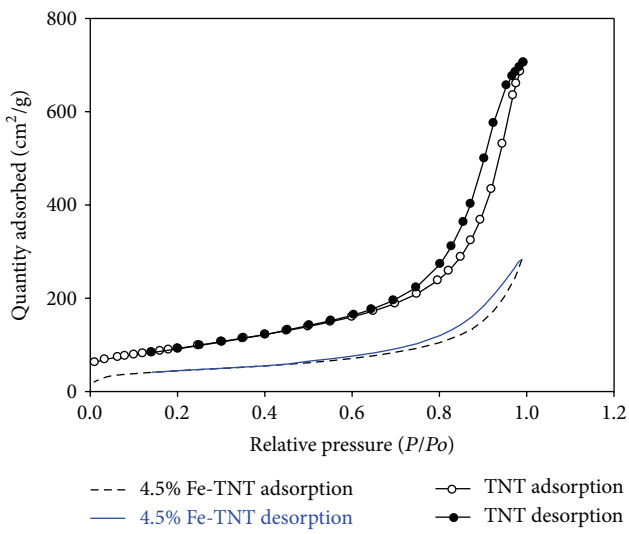

Figure 5: The curve of N_2 adsorption/desorption.

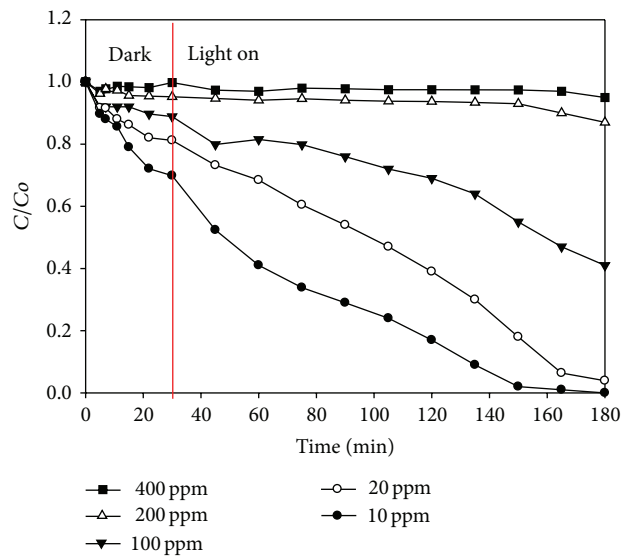

Figure 6: The effect of initial concentration on degradation efficiency under 254 nm UV and 1.13 % Fe-TNT of 0.04 gL^{-1}.

It can be seen that the photodegradation efficiency of methylene blue was inversely proportional to its concentration, which means that the lower the dye concentration, the higher the efficiency of the dye photodegradation [21]. In addition, the degradation efficiency of the MB decreased with increasing solution concentration [20].

3.3.2. The Effect of Dye Species. The three types of dyes were analyzed in this study. The degradation results under UV light are shown in Figure 5. After 180 min, the degradation efficiency of MB reached 99%, but the degradation efficiency of RBK5 was only 68% under 254 nm with and 0.04 gL^{-1} of 1.13% Fe TNT. These phenomena can be explained by the chemical structure of RBK5.

The test results under illuminated UV light with the three types of dyes are shown in Figure 7. The photodegradation efficiency of the three dyes ranked in order was MB, RBK5, and DB22. The MB degradation efficiency reached almost 100% after 180 min, whereas, the DB22 decolorizing efficiency was only 38% after 180 min because the chemical bonds of DB22 are longer. To increase degradation efficiency, length of exposure to UV light needs to be increased.

3.3.3. The Effect of Fe Content. The photocatalytic degradation of methylene blue (MB, 10 ppm) by 0.77–4.5 wt% Fe-doped TNT was conducted under a 14-W UV and visible light. The power of a 14-W UV and visible light is a very low source compared to conventional visible sources or solar light at 300–500 watts [22]. The 1.13% Fe TNT displayed the best properties in this experiment, as shown in Figure 8. The photodegradation efficiency abruptly decreased to 62% due to an agglomeration and sedimentation of the catalyst

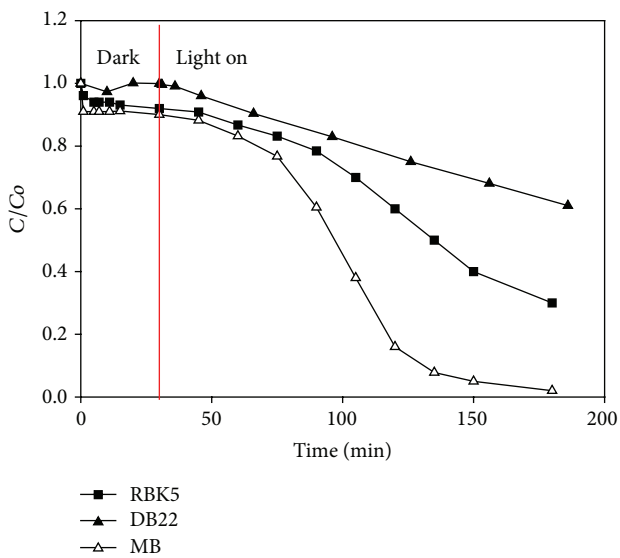

Figure 7: The effect of dye species on degradation efficiency under 254 nm UV and 1.13% Fe TNT of 0.04 gL^{-1}.

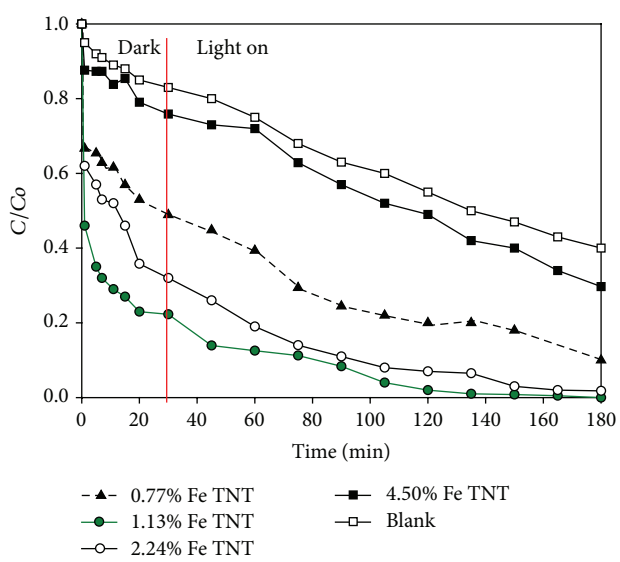

Figure 8: The effect of Fe content on degradation efficiency under 254 nm UV and catalysts loading of 0.04 gL^{-1}.

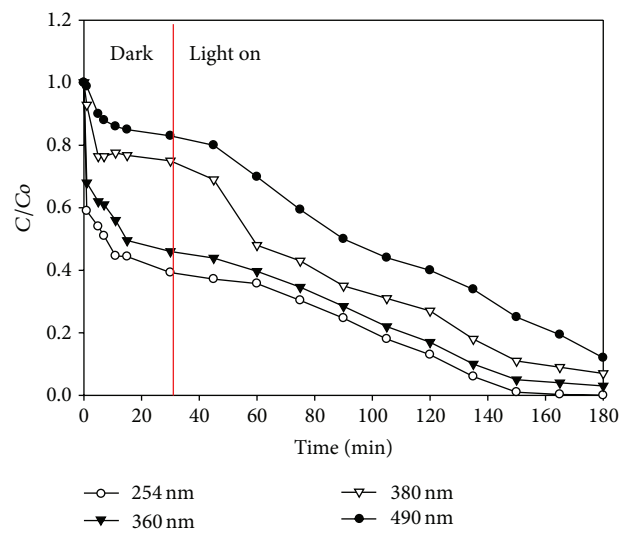

Figure 9: The effect of light source on degradation efficiency for 10 ppm MB removal and catalysts loading of 0.04 gL^{-1} with 1.13% Fe TNT.

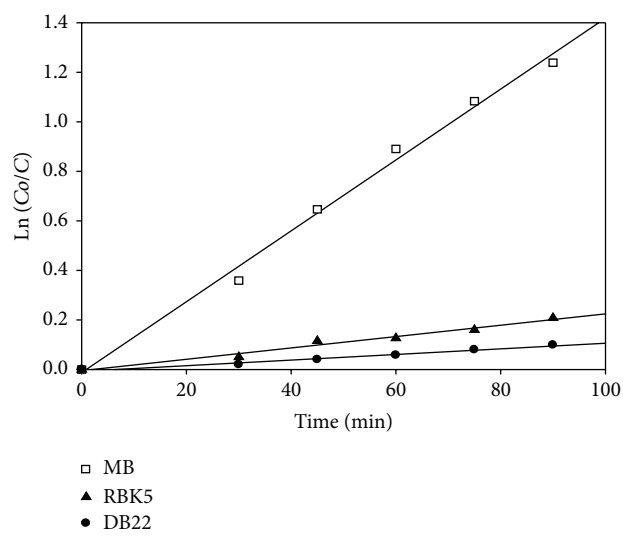

Figure 10: Pseudo-first-order kinetics plot for decolorization of 10 ppm MB, RBK5, and DB22 with 0.13 gL^{-1} catalyst under 254 nm light source.

particles when the Fe content exceeded 4.50%. This caused an increase in the particle size and a decrease in a specific surface area which lead to a decrease in the number of surface active sites [23].

El-Sharkawy et al. [24]. indicate that MB was not degraded completely when irradiated with UV in the absence of catalyst after 25 hr. This study has the same r.

3.3.4. The Effect of Light Source. There are four kinds of light sources, including 254 nm UV, 365 nm, 380 nm, and 490 nm light, for assessing the effect of light sources. The decolorizing efficiency reached almost 100% after 180 min of illumination time under 254 nm UV, as shown in Figure 9. Decolorizing efficiency reached 90% after 180 min under near visible light (λ = 380 nm). In addition, the decolorizing efficiency was 95% under 365 nm UV. Several minutes were spent before each reaction to maintain the temperature stability. The temperature was kept at 25°C by constant temperature water bath circulation system.

3.3.5. Kinetic Analysis. The photocatalytic degradation of MB, RBK5, and DB22 dyes as a function of the irradiation time was observed to follow an exponential decay as depicted in Figure 10. These results suggest that the photodegradation reaction follows the pseudo-first-order reaction kinetics. The pseudo-first-order reaction rate constant and half-life

Table 1: Pseudo-first-order kinetic parameters of different dyes.

Catalyst	R^2	k_1 (min^{-1})	$t_{1/2}$ (min)
MB	0.993	0.014	49.5
RBK5	0.937	0.005	21.0
DB22	0.947	0.002	18.3

parameters for MB dyes are listed in Table 1. The values of R^2 for different dyes show that a good compliance with the pseudo-first-order equation and the regression coefficients for the linear plots all exceeded 0.94.

4. Conclusion

In this study, the characterization of TNT and Fe TNT prepared using a hydrothermal and photodeposition method was performed. The time of decolorization increased with an increase in the initial MB concentration. The decolorizing efficiency decreased with increasing initial MB concentration, and a higher efficiency was obtained under UV-light illumination. However, excessive loading decreased the efficiency, and 1.13% weight Fe loading was found to be the optimal addition. Fe TNT using different Fe loadings was well characterized by the pseudo-first-order kinetic model.

Acknowledgment

Financial support from the National Science Council through Grant NSC-100-2622-E-562-002-CC3 and NSC-101-2221-E-562-003-MY3 is gratefully acknowledged.

References

[1] N. M. Mahmoodi and M. Arami, "Decolorization and aromatic ring degradation kinetics of Direct Red 80 by UV oxidation in the presence of hydrogen peroxideutilizing TiO_2 as a photocatalyst," *Chemical Engineering Journal*, vol. 112, pp. 191–196, 2005.

[2] Q. Zhang, "Photocatalytic degradation of methyl blue dye by pure and Platinum doped Titanium Dioxide Nanotube photocatalysts," *Advanced Science Letters*, vol. 18, no. 8, pp. 213–220, 2012.

[3] N. Daneshvar, A. Oladegaragoze, and N. Djafarzadeh, "Decolorization of basic dye solutions by electrocoagulation: an investigation of the effect of operational parameters," *Journal of Hazardous Materials*, vol. 129, no. 1–3, pp. 116–122, 2006.

[4] C. Pan and Y. Zhu, "New Type of $BiPO_4$ Oxy-acid salt photocatalyst with high photocatalytic activity on degradation of dye," *Environmental Science and Technology*, vol. 44, no. 14, pp. 5570–5574, 2010.

[5] Y. Hu, Y. Tang, X. Tang, H. Li, and D. Liu, "The photocatalytic degradation of methylene blue in wastewater by nano-structured Cr-doped TiO_2 under low power visible-light irradiation," in *Proceedings of the 5th International Conference on Bioinformatics and Biomedical Engineering (iCBBE '11)*, May 2011.

[6] S. P. Kamble, S. B. Sawant, and J. C. Schouten, "Photocatalytic and photochemical degradation of aniline using concentrated solar radiation," *Journal of Chemical Technology and Biotechnology*, vol. 78, pp. 865–872, 2003.

[7] Y. Wang, J. Li, P. Peng, T. Lu, and L. Wang, "Preparation of S-TiO_2 photocatalyst and photodegradation of L-acid under visible light," *Applied Surface Science*, vol. 254, no. 16, pp. 5276–5280, 2008.

[8] V. Štengl, F. Opluštil, and T. Nemec, "In^{3+}-doped TiO_2 and TiO_2/In_2S_3 nanocomposite for photocatalytic and stoichiometric degradations," *Photochemistry and Photobiology*, vol. 88, no. 2, pp. 265–276, 2012.

[9] Y. Hu, Y. Tang, X. Tang, H. Li, and D. Liu, "The photocatalytic degradation of methylene blue in wastewater by nano-structured Cr-doped TiO_2 under low power visible-light irradiation," in *Proceedings of the 5th International Conference on Bioinformatics and Biomedical Engineering (iCBBE '11)*, May 2011.

[10] A. Fujishima and K. Honda, "Electrochemical photolysis of water at a semiconductor electrode," *Nature*, vol. 238, no. 5358, pp. 37–38, 1972.

[11] C. Zhang, L. Gu, Y. Lin, Y. Wang, D. Fu, and Z. Gu, "Degradation of X-3B dye by immobilized TiO_2 photocatalysis coupling anodic oxidation on BDD electrode," *Journal of Photochemistry and Photobiology A*, vol. 207, no. 1, pp. 66–72, 2009.

[12] C. C. Tsai, *Structure analysis of nanotubes synthesized from hydrothermal treatment on TiO_2 [Ph.D. thesis]*, National Cheng Kung University Department of Chemical Engineering, Tainan City, Taiwan, 2005.

[13] M. Boroski, A. C. Rodrigues, J. C. Garcia, L. C. Sampaio, J. Nozaki, and N. Hioka, "Combined electrocoagulation and TiO_2 photoassisted treatment applied to wastewater effluents from pharmaceutical and cosmetic industries," *Journal of Hazardous Materials*, vol. 162, no. 1, pp. 448–454, 2009.

[14] K. V. Kumar, K. Porkodi, and F. Rocha, "Langmuir-Hinshelwood kinetics-a theoretical study," *Catalysis Communications*, vol. 9, no. 1, pp. 82–84, 2008.

[15] M. H. Habibi, A. Hassanzadeh, and S. Mahdavi, "The effect of operational parameters on the photocatalytic degradation of three textile azo dyes in aqueous TiO_2 suspensions," *Journal of Photochemistry and Photobiology A*, vol. 172, no. 1, pp. 89–96, 2005.

[16] S. Song, J. Tu, Z. He, F. Hong, W. Liu, and J. Chen, "Visible light-driven iodine-doped titanium dioxide nanotubes prepared by hydrothermal process and post-calcination," *Applied Catalysis A*, vol. 378, no. 2, pp. 169–174, 2010.

[17] J. G. Yu, H. G. Yu, C. H. Ao, S. C. Lee, J. C. Yu, and W. Ho, "Preparation, characterization and photocatalytic activity of in situ Fe-doped TiO_2 thin films," *Thin Solid Films*, vol. 496, no. 2, pp. 273–280, 2006.

[18] D. Park, T. Sekino, S. Tsukuda, and S. Tanaka, "Synthesis of Sm-doped TiO_2 nanotubes and analysisof their methylene blue-removal properties under dark and UV-irradiated conditions," *Research on Chemical Intermediates*, vol. 39, no. 4, pp. 1581–1591, 2013.

[19] S. Song, J. Tu, Z. He, F. Hong, W. Liu, and J. Chen, "Visible light-driven iodine-doped titanium dioxide nanotubes prepared by hydrothermal process and post-calcination," *Applied Catalysis A*, vol. 378, no. 2, pp. 169–174, 2010.

[20] C. T. Hsieh, W. S. Fan, W. Y. Chen, and J. Y. Lin, "Adsorption and visible-light-derived photocatalytic kinetics of organic dye on Co-doped titania nanotubes prepared by hydrothermal synthesis," *Separation and Purification Technology*, vol. 67, no. 3, pp. 312–318, 2009.

[21] R. M. Mohamed, I. A. Mkhalid, E. S. Baeissa, and M. A. Al-Rayyani, "Photocatalytic degradation of methylene blue by

Fe/ ZnO/SiO_2 nanoparticles under visible light," *Journal of Nanotechnology*, vol. 2012, Article ID 329082, 5 pages, 2012.

[22] Y. Hu, Y. Tang, X. Tang, H. Li, and D. Liu, "The photocatalytic degradation of methylene blue in wastewater by nano-structured Cr-doped TiO_2 underlow power visible-light irradiation," in *Proceedings of the 5th International Conference on Bioinformatics and Biomedical Engineering (iCBBE '11)*, pp. 1–4, School of Technical Physics, Xidian University, Shaanxi, China, 2011.

[23] D. Zhao, J. Wang, Z. Zhang, and J. Zhang, "Photocatalyticdegradation of omethoate using NaY zeolite-supported TiO_2 ," *Frontiers of Chemical Engineering in China*, vol. 3, no. 2, pp. 206–210, 2009.

[24] E. A. El-Sharkawy, A. Y. Soliman, and K. M. Al-Amer, "Comparative study for the removal of methylene blue via adsorption and photocatalytic degradation," *Journal of Colloid and Interface Science*, vol. 310, no. 2, pp. 498–508, 2007.